

## ELECTRON ACCELERATION AND EXCITATION PROCESSES IN THE VICINITY OF A MERCURY DISCHARGE CONSTRICTION\*

S. FAZLIAN<sup>1\*\*</sup>, S. SOBHANIAN<sup>1</sup> AND A. MURADOV<sup>2</sup>

<sup>1</sup>Faculty of Physics, University of Tabriz, Tabriz, I. R. of Iran, Email: fazlian@tabrizu.ac.ir

<sup>2</sup>Physics Dept., Baku State University, Baku, Azerbaijan

**Abstract** – In the present paper axial distributions of plasma and floating potentials, electron and ion densities and EEDF have been measured in the DL region of a Hg discharge constriction. An attempt has been made for the resolution of opposing charged layer structures in DL. Excitation processes in the constriction region are studied. Using the linearization method for the nonstationary balance equations system and choosing appropriate discharge conditions, the step excitation rate by the electron impact for  $6^3P_2 \rightarrow 7^1S_0$  transition in Hg is determined.

**Keywords** – Double layers (DL), EEDF, plasma parameters, excitation processes, constriction edge, excitation rates, modulation depths, spectral lines

### 1. INTRODUCTION

Double layers (DL) in plasma have been studied by many authors. Interest in this problem arises from different important subjects like: mono-and duoplasmatron ion sources, high intensity light emission sources, high current discharges, astrophysics experiments and their laboratory modeling [1-6]. DL represents the space charge region of order of tens to hundreds of Debye lengths. In this region the sudden change in potential occurs due to the space charge separation. The resulting electric field from the Poisson equation imparts additional energies to electrons. Electrons are accelerated towards the higher potential side, and thus change the shape of electron energy distribution function (EEDF). Some occur in the ionization and excitation processes.

The simplest and most interesting (due to its applications) way of obtaining DL in plasma are to create sharp changes in the diameter of the positive column of the low pressure discharge [7-9]. In such discharge tubes, each part has its own potential distribution, and it is only near the constriction region where the sharp changes occur in potential.

The DL formed at the change of discharge tube diameter has been studied in He [8]. Axial distributions of plasma potential, electron density and EEDF have been measured in the constriction region. Double humped distribution functions were obtained. EEDFs were calculated from the kinetic equation using measured profile of potential when momentum-transfer quasielastic collision frequency is significantly higher than inelastic collision frequency and the characteristic scale is much longer than the electron mean free path. Axial distributions of different types spectral line intensities were measured. The numbers of excitations and ionizations were calculated on the base of measured distributions.

---

\*Received by the editor July 1, 2003 and in final revised form August 24, 2005

\*\*Corresponding author

A double hump in EEDF due to the installation of an orifice has been also observed in an Hg-Ar mixture collision controlled positive column [9]. A one dimensional model has been introduced to explain this EEDF by taking into account the absence of local equilibrium between the electrons and the electric field. A solution of the Boltzmann equation, including the spatial derivative under the assumption of a rectangular-shaped electric field, has successfully predicted a partial shift of low energy electrons to higher energies. It was shown that the region of energy gain and energy loss are separated in space. This feature is a substantial deviation from the conventional positive column discharge where energy deposition and energy dissipation always go hand in hand.

Recently the spatial variations of plasma parameters were detected in both axial and radial directions by installing a mesh-grid in an homogeneous He positive column [10]. EEDF has been measured and double-humped distributions were obtained. The spatial variation of radiation intensity is also detected by image reconstruction using a computerized tomography technique. The downstream variations of EEDF are calculated from the kinetic equation solution using the Fourier transform method.

One can note that although kinetics of electron acceleration and the physical properties of the constriction are well understood, to our knowledge the structure of opposing charged layers has not been analyzed and its connection to EEDF has not been investigated. On the other hand, the special shape of EEDF and different energy dependence of cross sections of singlet and triplet levels may cause some peculiarities in excitation processes in the constriction region.

In the present paper, axial distributions of plasma and floating potential, electron and ion densities, and EEDF have been measured in the DL region in the Hg discharge constriction. An attempt has been made for the resolution of opposing charged layer structures. Excitation processes in the constriction region are studied. By using the linearization method for the nonstationary balance equation system [11] and choosing appropriate discharge conditions, the step excitation rate in Hg is determined.

## 2. EXPERIMENTAL ARRANGEMENT AND RESULTS OF STATIONARY MEASUREMENTS

Experiments were carried out in the positive column of a hot cathode discharge in Mercury vapour. The discharge tube is composed of two cylindrical glass tubes of different diameters, 55 mm and 18 mm (Fig. 1). The discharge was maintained between a directly heated tungsten filament in the wide part of the tube and a conic shaped nickel anode placed in the movable narrow part of the tube. A movable Langmuir probe, which provides radial distribution measurements of plasma parameters, is placed into the discharge tube. The DL position, with respect to the probe or monochromator's slit, could be changed by moving the anode placed in the narrow part of the tube, with the help of a magnet. The measurements were carried out in Mercury vapour at room temperature ( $P=1.2 \times 10^{-3}$  Torr) in the discharge current range from 20 mA to 600 mA.

EEDF and electron number density were measured by the method of the second derivative of the probe characteristic [12]. An amplitude modulated RF signal is superimposed on probe bias. The amplitude of the modulating harmonic of the probe current is plotted versus the probe bias voltage. This curve represents the second derivative of the probe characteristic and is proportional to EEDF. Plasma potential was determined at the zero value of the second derivative. Electron number density was determined from the probe current at plasma potential.

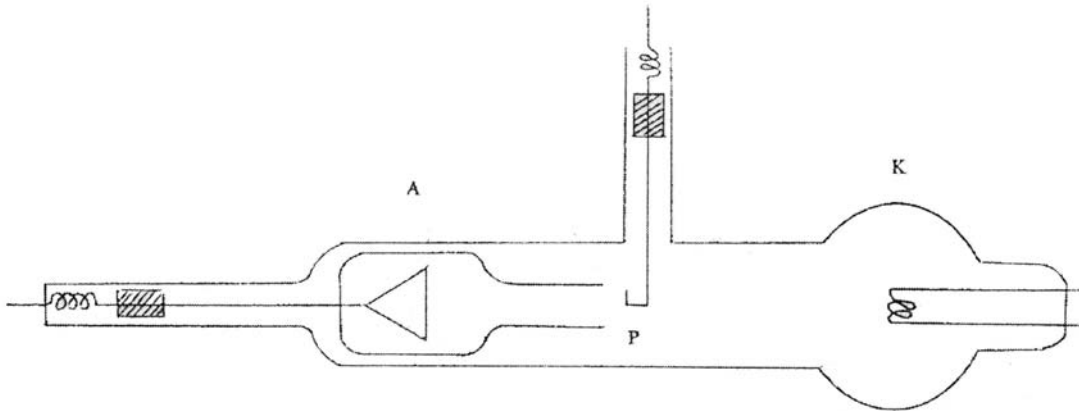


Fig. 1. Discharge tube constriction scheme. A- movable conic shaped anode, K-Cathode, P-movable Langmuir probe

Ion number density was determined from the ion part of probe characteristics. At sufficient high negative probe potential relative to plasma potential (determined as a zero point of second derivative) the probe current is given as [13]:

$$I = \frac{2}{9} \sqrt{\frac{2e}{M}} \frac{LV^{3/2}}{r\beta^2} \quad (1)$$

Here  $r$ ,  $L$  and  $V$  are the radius, probe length and probe voltage, respectively.  $M$  is the ion mass and  $e$  its charge. The parameter  $\beta^2$  is associated to the ratio of sheath radius to probe radius. Its value was obtained from Eq. 1 using the measured probe ion current. The sheath and probe radii ratio was taken from the tables in [13]. Ion number densities  $n_i$  were calculated from the ion current expression in the case of cylindrical probe:  $I_i = 0.4n_i eV_i S$ . Here  $V_i = (kT_e/M)^{1/2}$  is the ion velocity at the sheath edge,  $S$  is the sheath area.

Spectral line intensities were measured in a transverse direction without taking into account the radial distribution of plasma parameters.

The discharge constriction region, axial distribution of electron and ion number densities, plasma potential and floating potential distributions at discharge current value 200 mA are shown in Fig. 2. As seen from this Figure, near the constriction, electron and ion densities increase sharply at first and then fall to density levels of the narrow part. Electron and ion densities are shifted, as a whole, towards the anode side with respect to the potential drop (maximum electric field). Electrons are accelerated through the DL and gain additional energies. The number of ionization is thus increased, resulting in the increase of charged particles densities towards the higher potential region. The electron density distribution curve is shifted towards the cathode relative to the ion distribution curve. Axial distribution of plasma potential  $V_p$  and floating potential  $V_0$  are also shown on the same Figure. The changes in difference between  $V_p$  and  $V_0$  are due to the significant changes in EEDF shape.

DL is a spherical segment formed near the constriction, and the accelerated electrons are focused towards the narrow part. Radial distributions of charged particles in the vicinity of the constriction are significantly narrower than those for the regions far from the DL.

EEDF and potential distribution measurement at different discharge currents showed no changes in the potential drop and EEDF shape for the current range of 20 mA to 600 mA. Accordingly, the increase in discharge current leads to the increase of absolute ion and electron densities, while EEDF shape and excitation regimes remain the same. EEDF measured at distances of 10 mm and 12 mm from the constriction edge towards the cathode side are shown in Fig. 3. Additional maximum in EEDF corresponds to the electrons accelerated in DL. As one can see, the shift of the probe position towards the anode leads to the shift of the additional maximum towards the higher energies and to the decrease in its value.

Numbers of excitations of triplet and singlet levels were calculated from the measured EEDF and cross-sections data [14]. Results of calculations for the  $7^3S_1$  and  $6^1D_2$  levels are shown in Fig. 4. Axial distributions of relative intensities of spectral lines  $\lambda=404.6$  nm and  $\lambda=579.1$  nm are shown on the same Figure. As is seen, these curves are shifted relative to each other and their intensities reach their maximum at different distances from the constriction. The change in excitation regimes of triplet and singlet levels results from the shift in the second maximum position on EEDF and from the different energy dependences of the corresponding level's cross-sections.

The discrepancy between calculation and measured intensities can be explained by the fact that the radial distribution has been neglected. This would give the difference between the calculated intensities at the tube centre and the measured intensities across the tube cross-section (integrated along the diameter). Similar changes were observed in the population relation for other triplet and singlet levels, taking into account changes due to their different threshold energies. Thus it is possible to create a local partial preferable selective population of some levels using the changes in the excitation rates of different type levels in the positive column constriction.

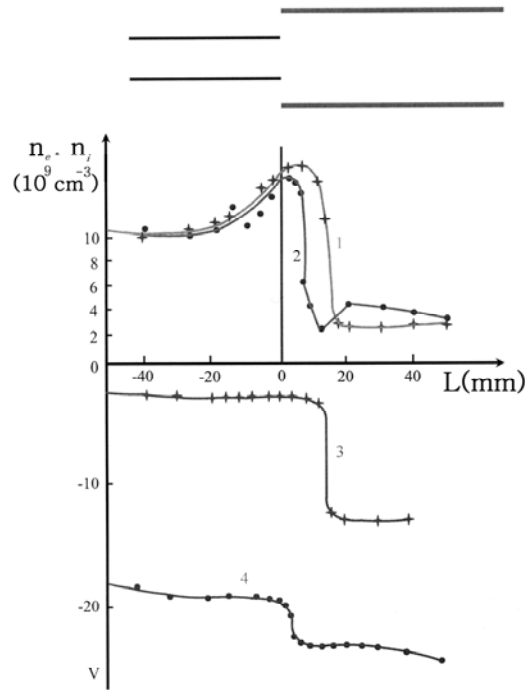


Fig. 2. Distributions of plasma parameters as a function of distance from the constriction edge: 1. Electron number density, 2. Ion number density, 3. Plasma potential and 4. Floating potential, constriction region is shown on the upper part of the Fig.

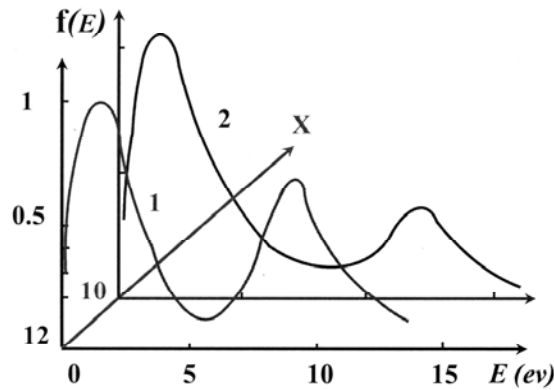


Fig. 3. EEDF,  $f(E)$ , measured at distances of 10 mm (curve 2) and 12 mm (curve 1) from the constriction edge

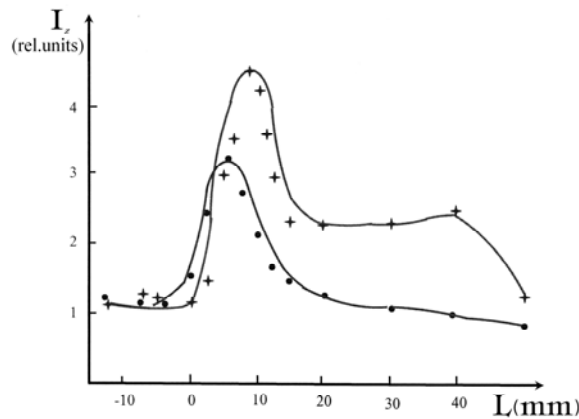


Fig. 4. Axial distributions of relative intensities of spectral lines: (+) for  $\lambda=404.6$  nm and (.) for  $\lambda=579.1$  nm. Points are results of calculated numbers of excitations for the  $7^3S_1$  and  $6^1D_2$  levels respectively

### 3. DETERMINATION OF STEP EXCITATION RATE OF HG IN NONSTATIONARY DISCHARGE CONSTRICTION

The existence of a shifting hump on EEDF and changes in excitation rates of different type levels can be used for simple determination of step excitation rates. These rates, as well as the corresponding cross-sections, are very important in atomic spectroscopy and plasma physics. There is little experimental data on this subject, and calculated theoretical results are commonly used for different studies. Such a calculation has been performed and recently reported for He [15].

Let us consider the system of balance equations for two levels. One of them is metastable ( $m$ ), which is excited only directly by electron impact. The other one is excited not only directly, but also by step excitation from the metastable levels. The balance equations may be written as:

$$\frac{dN_m}{dt} = N_0 n_e \alpha_{0m} - (n_e \beta_m + \tau_m^{-1}) N_m \quad (2)$$

$$\frac{dN_k}{dt} = N_0 n_e \alpha_{0k} + N_m n_{mk} - N_k A_k \quad (3)$$

Here  $N_0$ , and  $n_e$  are, respectively, neutral atom and electron number densities;  $N_m$ ,  $N_k$  are populations of considered levels,  $\alpha_{0m}$ ,  $\alpha_{0k}$  are direct excitation rates,  $\alpha_{mk}$  and  $\beta_m$  are step excitation and loss rate coefficients for metastable atoms due to electron impact,  $\tau_m$  is the diffusion time of metastable atoms to the walls of the tube, and  $A_k$  is the spontaneous transition probability. It is assumed that metastable atoms are lost by means of electron impact transition to neighboring levels, and by diffusion to the discharge tube walls. The second level is lost as a result of spontaneous transition to lower levels.

Let us assume plasma parameters oscillations in the form of:

$$n_e(t) = n_0 + n_1 e^{i\omega t}; N_m(t) = N_{m0} + N_{m1} e^{i\omega t}; N_k(t) = N_{k0} + N_{k1} e^{i\omega t} \quad (4)$$

Here subscripts 0 and 1 denote the unperturbed values and complex amplitudes of plasma parameters. If  $|n_1| \ll n_0$ ,  $|N_{m1}| \ll N_{m0}$ ,  $|N_{k1}| \ll N_{k0}$ , the equations (2,3) are linearized as:

$$i\omega N_{m1} = N_0 n_1 \alpha_{0m} - (n_0 \beta_m + \tau_m^{-1}) N_{m1} - n_1 \beta_m N_{m0} \quad (5)$$

$$i\omega N_{k1} = N_0 n_1 \alpha_{0k} + (N_{m0} n_1 + N_{m1} n_0) \alpha_{mk} - N_{k1} A_k \quad (6)$$

Equations (5) & (6) represent the complex amplitudes of oscillating plasma parameters. At  $\omega \rightarrow 0$  these equations are simplified as:

$$N_0 n_1 \alpha_{0m} - (n_0 \beta_m + \frac{1}{\tau}) N_{m1} - n_1 \beta_m N_{m0} = 0 \quad (7)$$

$$N_0 n_1 \alpha_{0k} + (N_{m0} n_1 + N_{m1} n_0) \alpha_{mk} - N_{k1} A_k = 0 \quad (8)$$

From these equations one can obtain:

$$\eta_{k1} = \eta_n \left( 1 + \frac{N_{m0}^2}{N_0 \alpha_{0m} I_{k0} \tau_m} \alpha_{mk} \right) \quad (9)$$

Here  $I_{k0} = N_{k0} A_{k0}$ ,  $\eta_{k1} = \frac{N_{k1}}{N_{k0}}$ , and  $\eta_n = \frac{n_1}{n_0}$  are the modulation depths of spectral line intensity and electron density.

As it is seen from Eq. 9, one can obtain  $\alpha_{mk}$  by plotting  $\eta_{k1} - \eta_n$  versus  $\eta_n$ . Populations  $N_{m0}$ ,  $N_0$  and  $I_{k0}$  are measurable quantities, and direct excitation rate  $\alpha_{0m}$  and diffusion time  $\tau_m$  can be calculated.

Electron density measurements for different discharge currents at different points showed that at low frequencies, electron density modulation depth is equal to the discharge current modulation depth in a wide range of discharge currents. Thus in Eq. (9),  $\eta_n$  is replaced by  $\eta_j$ , the current depth for simplifying purposes.

In the stationary case of Eq. 2, at low discharge currents and low electron densities, only diffusion to the tube's wall remains in the metastable atom's loss term. Due to the proportionality of the creation rate of metastable atoms with electron density,  $N_m$  increases linearly by increasing discharge current. At high electron densities the diffusion term can be neglected, the gain and loss rates of metastable atoms become proportional to electron density, and  $N_m$  remains invariant with respect to the increase of discharge current.

The dependences of  $6^3P_0$  and  $6^3P_2$  level populations measured at a distance of 12 mm to the cathode side from the constriction edge are shown in Fig. 5. Measurements of populations were

performed on the base of  $\lambda = 404.6$  nm and  $\lambda = 546.0$  nm line absorption. It can be seen that the  $6^3P_0$  level population is saturated at 350 mA and that of the  $6^3P_2$  level at  $J_p = 200$  mA .

To determine the step excitation rate, the discharge current was modulated at a frequency of 63 Hz. This frequency was lower than all characteristic frequencies in the discharge and satisfies  $\omega \rightarrow 0$  condition. To obtain appreciable modulation depth of  $6^3P_2$  levels population, and to reach the situation where its role on step excitation at the current modulated regime is more significant, discharge currents were taken within a 200 mA range.

The dependence of  $\eta_{k1} - \eta_j$  on  $\eta_j$  for  $\lambda = 407.7$  nm line is shown in Fig. 6. Other quantities in Eq.9 are represented in Table 1. The value of  $\alpha_{mk}$  for the transition  $6^3P_2 - 7^1S_0$ , determined from Eq.9, is also shown in this Table. The calculated rate of this transition using the first Born approximation [16] is given in the last column.

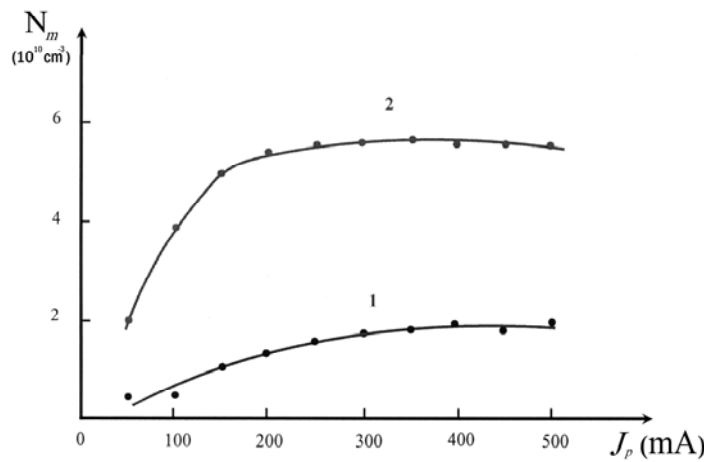


Fig 5. The dependencies of  $6^3P_0$  (curve 1) and  $6^3P_2$  (curve 2) level populations on discharge current at the 12 mm from the constriction edge

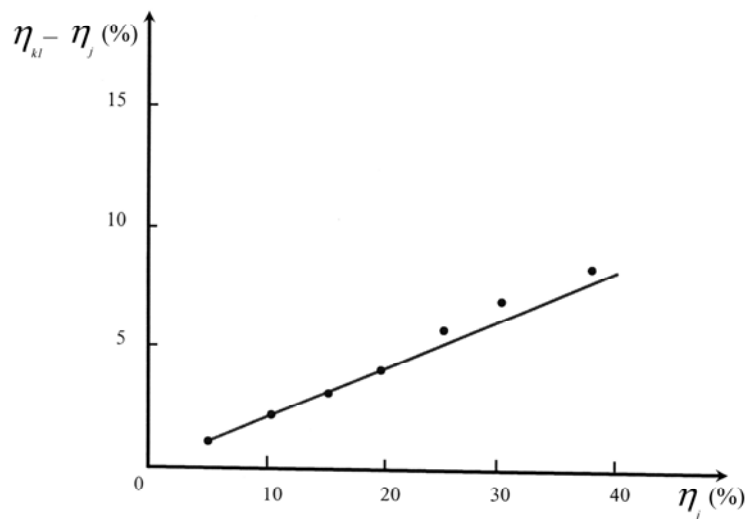


Fig 6. The dependence of  $\eta_{k1} - \eta_j$  on  $\eta_j$  for the spectral line  $\lambda = 407.7$  nm.

$J_p = 200$  mA,  $L = 12$  mm. Current modulation frequency  $\nu = 63$  Hz

Table 1. The experimental and calculated values of transition rates

$J_p$ (mA)	$n_0$ ( $cm^{-3}$ )	$N_{m0}$ ( $6^3 P_2$ ) $cm^{-3}$	$N_0$ ( $6^1 S_0$ ) $cm^{-3}$	$\alpha_{0m}$ ( $6 P_2$ ) $cm^3 s^{-1}$
200	$1.2 \times 10^{10}$	$1.1 \times 10^{11}$	$4 \times 10^{13}$	$8.1 \times 10^{-8}$
$I_{K0}$ ( $cm^{-3} S^{-1}$ )	$\tau_m$ (S)	$\Delta(\eta_{k1} - \eta_j) / \Delta\eta_j$	$\alpha_{mk}$ (exp.) $cm^3 s^{-1}$	$\alpha_{mk}$ (calc.) $cm^3 s^{-1}$
$2.1 \times 10^{14}$	$1.3 \times 10^{-5}$	0.2	$1.4 \times 10^{-7}$	$0.57 \times 10^{-7}$

#### 4. CONCLUSIONS

As can be seen, the experimental value for the transition rate is higher than the calculated one. This discrepancy may be the result of neglecting transitions from  $6^3 P_0$ ,  $6^3 P_1$  and  $6^1 P_1$  levels. These levels, which do not have an appreciable contribution to step excitation in the stationary case, can not reach the saturation. They have high modulation depth for a wide range of discharge current, so it is possible that they have a considerable contribution in the current modulated regime. Furthermore, the transition rate calculations were performed for the Maxwellian distribution, while the measured EEDFs were double humped distributions, which is very different from the Maxwellian case.

#### REFERENCES

1. Lavrov, B. P. & Simonov, V. Y. (1978). Anode Space-Charge Sheath in The Monoplasatron and Duoplasmatron. *Journ of Techn. Phys. (Soviet Physics)* 48(8). 1744-1746.
2. Lavrov, B. P. & Shitashka, L. P. (1979). Capillary-Arc Light Source Employing Mixture of Deuterium with Neon. *J. of Opt. Technology*. 46(11), 58-59.
3. Lutsenko E. I., Sereda, N. D. & Kontsevov, L. M. (1975). Current Restrictions in a High Current Discharge. *J. of Experimental & Theoretical Physics (JETP)*, 2067-78
4. Block, L. (1978). A Double Layer Review. *Astrophys. & Space Sci.* 55, 59-83.
5. Torven, S. & Lindberg, L. (1980). Properties of a Fluctuating Double Layer in a Magnetized Plasma Column. *J. Phys. D: Appl. Phys.*, 13, 2285-3000.
6. Raadu, M. & Carlquist, P. (1981). Electrostatic Double Layers and Plasma Evaluation Process. *Astrophys. Space Sci.*, 74, 189-206.
7. Anderson, D. J. (1977). Measurement of Electron Energy Distributions in Front and Behind of a Stationary plasma. *J. of Phys. D: Appl. Phys.*, 10(12), 1549.
8. Huseinov, T. H. & Muradov, A. H. (1991). Electron Impact Excitation Transfer Between  $7^3 S_1 - 7^1 S_0$  State of Hg in Nonstationary Double Layer. *J. of Techn. Phys.*, 61(5), 130-131.
9. Godyak, V., Lagushenko, R. & Maya, J. (1988). Spatial Evaluation of The Electron Energy Distribution in the Vicinity of a Discharge-Tube Constriction. *J. of Physics Phys. Rev. A.*, 38(4), 2044-2055.
10. Ohe, K. & Yamada, H. (1994). Distribution of Plasmas Due to Installation of a Grid in Homogeneous He Positive Column. *J. Phys. D: Appl. Phys.*, 27(4), 756-764.
11. Muradov, A. H. (1988). Dynamical Study of Ionization-Recombination Regime. *Radiophysics Vol.* 31(6), 763-766.
12. Vorobyova, N. A., Kagan, Y. M. & Milenin, V. M. (1964). The Electron Distribution Function in a positive Column Discharge in Ne and He. *J. of Technical Phys.* 34, 2079.
13. Kaptsov, N. A. (1947). Electricity in gases and vacuum. *M. L.*
14. Zapesochniy, I. P. & Shpennik, O. B. (1966). *JETP*, 50(4), 890.

15. Shevelko, V. P. & Tawara, H. (1995). Cross Sections for Electron-Impact Induced Transition Excited States in He. *NIFS-DATA-28. Nagoya*
16. Vaynshtein, L. A., Sobelman, I. I. & Yukov, E. A. (1974). *Cross-Sections of Atoms and Ions*. Nauka.